Cumulus Parameterization and Rainfall Rates II

T. N. KRISHNAMURTI, SIMON LOW-NAM AND RICHARD PASCH

Department of Meteorology, Florida State University, Tallahassee, FL 32306

(Manuscript received 15 June 1982, in final form 5 January 1983)

ABSTRACT

In the various formulations of Kuo (1965, 1974) type cumulus parameterization schemes, the moistening and heating by the cumulus are made proportional to the humidity and temperature differences between a model cloud and its environment. The constants of proportionality that differentiate the various versions of the Kuo's schemes are based on different closure assumptions. The proportion of available moisture supply that goes into the moistening by cumulus convection usually determines these constants. It is possible to diagnostically calculate the observed (or what might be called the exact) measures of these constants of proportionality. This enables one to define an ultimate Kuo scheme where the vertical integrals of the heating and moistening are exactly known but the vertical distributions are limited by the aforementioned structure functions. This ultimate Kuo scheme is not a prognostic scheme, but it serves as a benchmark in defining how far one can progress with this type of scheme in the prognostic sense. Using the final validated GATE B-scale data sets a comparison is made between the observed vertical distributions of the apparent heat source and apparent moisture sink (obtained from direct substitutions of observed data) with the ultimate Kuo scheme to assess its scope. Comparison of Kuo (1965, 1974) type schemes is next carried out with the ultimate Kuo scheme to address their limitations.

A proposal for a mesoscale convergence parameter η and a moistening parameter b is made to overcome some of the limitations of the above schemes. Here a multiple regression search of large-scale parameters, using 72 map times of data, is carried out to determine these parameters via least-square minimization of errors. These are next used to determine the vertical structure of moistening and heating, for a semi-prognostic formulation. The results show that by using the vertical average of the large-scale upward vertical motion and the lower tropospheric relative vorticity in the multiple regression, it is possible to attain an accuracy close to that prescribed by the ultimate Kuo scheme. Detailed results on the vertical distributions of the heating and moistening and the rainfall rates for the entire third phase of GATE are presented in this paper.

1. Introduction

In a recent study, Krishnamurti *et al.* (1980, thereafter referred to as I) presented a comparison of rainfall rate estimates from semi-prognostic application (one time step forecasts) for various cumulus parameterization schemes. The observations from the GATE A/B-scale array of ships were used in this study. (A list of acronyms is presented in Table 1.) The GATE observations included the conventional upper air data from ships as well as the radar estimates of rainfall rates for the entire third phase of GATE (Hudlow and Patterson, 1979). The cumulus parameterization schemes included the convective adjustment methods (hard and soft), two versions of Kuo's (1965, 1974) parameterization schemes, and the Arakawa-Schubert scheme (1974) following the GATE application of Lord (1980). In the earlier work we did not examine the vertical distributions of moistening and heating by the parameterized cumulus-scale motions. The present paper addresses these vertical distributions, their limitations, and an improved method is presented here.

In I we noted that remarkable agreement between the observed and predicted rainfall rates were in fact possible from the Kuo and Arakawa-Schubert-Lord methods when they were applied to the high-quality GATE A/B-scale data sets and verified against the radar-rainfall estimates. Since the publication of that study, Lord (1982) recently published detailed results on the application of the Arakawa-Schubert cumulus parameterization scheme to the GATE data sets and showed a close correspondence in the semi-prognostic estimates of rainfall rates as well as in the Phase III time-averaged vertical distribution of the heating and moistening by cumulus-scale motions.

Our interest in this problem is motivated by our efforts on short-to-medium range numerical weather prediction over low latitudes (Krishnamurti *et al.*, 1979, 1981). Here we feel that semi-prognostic tests on the vertical distribution of heating and moistening by the cumulus-scale motions need to be presented against observed values at 24 h (or even 6 h) intervals. The present study addresses the results of such semi-prognostic tests, within the framework of a generalized Kuo-type scheme, which appears quite promising in the context of tropical weather prediction. The results of applications to short-to-medium range prediction will be presented in part III of this study.

TABLE 1. List of acronyms.

GARP	Global Atmospheric Research Program
GATE	GARP Atlantic Tropical Experiment
FGGE	First GARP Global Experiment
Phase III	The period between 1 and 18 September 1974
A/B-scale	An array of six ships on a hexagonal array over the tropical eastern Atlantic Ocean
B-scale	An inner (inside the A/B scale) array of six ships in a hexagonal array over the tropical eastern Atlantic Ocean
ECMWF	European Center for Medium Range Weather Forecasting

2. Formulation of cumulus parameterization

Following Krishnamurti *et al.* (1976), Kanamitsu (1975) and Molinari (1982), we define the large-scale supply of moisture I_L by the relation

$$I_L = \frac{1}{g}\int_{p_B}^{p_T} \omega \frac{\partial q}{\partial p}\, dp. \tag{1}$$

In addition, we shall introduce here an additional source of moisture supply $I_L\eta$, which may be considered as a nonmeasurable mesoscale (or subgrid-scale) supply. The parameter η will be determined from GATE observations subject to certain constraints requiring reasonable vertical distributions of heating and moistening and rainfall rates. The total supply of moisture is expressed by

$$I = I_L(1 + \eta). \tag{2}$$

The supply of moisture required to produce a cloud on a grid square is next defined by the relation (Krishnamurti *et al.*, 1976; Kanamitsu, 1975)

$$Q = \frac{1}{g}\int_{p_T}^{p_B} \frac{q_s - q}{\Delta\tau}\, dp + \frac{1}{g}\int_{p_T}^{p_B}\left[\frac{c_pT(\theta_s - \theta)}{L\theta\Delta\tau} + \omega\frac{c_pT}{L\theta}\frac{\partial\theta}{\partial p}\right]dp. \tag{3}$$

The first term on the right-hand side denotes the supply required to replace an environmental humidity distribution from q to that of a local moist adiabat q_s in a cloud formation time scale $\Delta\tau$; as in I it has been assigned a value of 20 min. The first part of the second term on the right-hand side of the above equation denotes the time required for the establishment of the temperature T_s of a local moist adiabat in the same time scale, where T is the ambient temperature. The second part of the second term denotes the moisture supply required to overcome the adiabatic cooling due to large-scale ascent. The third term in Eq. (3) enables a smooth transition between the convective heating in the conditionally unstable atmosphere and the large-scale condensation heating in the absolutely stable situation of saturated ascent. The absence of the third term leads to a mathematical singularity in the formulation of heating and moistening as the neutral state is approached: this is a problem which is quite apparent in Kuo (1965), and requires a quick remedy with actual application to numerical weather prediction. To show the smooth transition when this term is retained we note that as the neutral state is reached, T approaches T_s, q approaches q_s, and the potential temperature θ approaches its saturation value θ_s. At this stage we can write

$$Q_\theta = \frac{c_p}{L}\left(\frac{1}{g}\right)\int_{p_T}^{p_B}\left(\frac{p}{p_0}\right)^{R/c_p}\omega\frac{\partial\theta}{\partial p}\, dp \tag{4}$$

along the vertical, the moist static energy is constant in this state, i.e.,

$$gz_s + c_pT_s + Lq_s = \text{constant along } p,$$

where the subscript s denotes the moist adiabat. Thus

$$\frac{\partial}{\partial p}[gz_s + c_pT_s + Lq_s] = 0. \tag{5}$$

This leads to the relation

$$\frac{c_p}{L}\left(\frac{p}{p_0}\right)^{R/c_p}\omega\frac{\partial\theta_s}{\partial p} = -\omega\frac{\partial q_s}{\partial p}, \tag{6}$$

i.e.,

$$\left.\begin{aligned} Q_\theta &= I_\theta \\ a_\theta &= 1 \end{aligned}\right\}.$$

Thus the first law of thermodynamics in the neutral state reduces to

$$\frac{\partial\theta}{\partial t} + \mathbf{V}\cdot\nabla\theta = 0. \tag{7}$$

If the boundary layer, advective and radiative processes stabilize the atmosphere and if large-scale condensation were possible over saturated regions, then the transition evolves in a very smooth manner without a singularity. We shall denote the two terms on the right-hand side of the above equations by Q_q and Q_θ, i.e.,

$$Q = Q_q + Q_\theta. \tag{8}$$

It should be noted that Q_q and Q_θ are known functions of large-scale variables. We shall next introduce a parameter b, following Kuo (1974), such that the rainfall rate R and a moistening rate M may be expressed by the relations,

$$R = I(1 - b), \tag{9}$$

$$M = Ib. \tag{10}$$

The above relations may be written as

$$R = I_L(1 + \eta)(1 - b), \tag{11}$$

$$M = I_L(1 + \eta)b. \tag{12}$$

Thus, in this formulation there are two unknown parameters η and b that need to be determined for closure of the cumulus parameterization scheme. Again, following Kuo (1974), we shall define two additional parameters a_θ and a_q by the relations

$$a_\theta = \frac{I(1-b)}{Q_\theta} = \frac{I_L(1+\eta)(1-b)}{Q_\theta}, \tag{13}$$

$$a_q = \frac{Ib}{Q_q} = \frac{I_L(1+\eta)b}{Q_q}. \tag{14}$$

In a primitive equation model, the equations for the time rate of change of potential temperature and specific humidity may be written

$$\frac{\partial\theta}{\partial t} + \mathbf{V}\cdot\nabla\theta = -\omega\frac{\partial\theta}{\partial p} + \frac{1}{c_p}\left(\frac{p_0}{p}\right)^{R/c_p} H_c + H_R, \tag{15}$$

$$\frac{\partial q}{\partial t} + \mathbf{V}\cdot\nabla q = -\omega\frac{\partial q}{\partial p} + E - P, \tag{16}$$

where only the effects of convective heating H_c are presently considered. E denotes evaporation and P the precipitation. Following Kuo (1965), we shall assume that between the pressure levels p_T and p_B the evaporation is not explicitly included, i.e., $E = 0$ for $p_T \leq p \leq p_B$. We shall next propose the generalized Kuo schemes all of which have the same vertical structure functions for heating and moistening, i.e.,

Heating proportional to $\theta_s - \theta$,

Moistening proportional to $q_s - q$.

The proportionality factors will vary in the different formulations of the Kuo schemes. Thus, we shall express the first law and the moisture conservation law by the relations

$$\frac{\partial\theta}{\partial t} + \mathbf{V}\cdot\nabla\theta + \omega\frac{\partial\theta}{\partial p} = a_\theta\left(\frac{\theta_s-\theta}{\Delta\tau} + \omega\frac{\partial\theta}{\partial p}\right) + H_R, \tag{17}$$

$$\frac{\partial q}{\partial t} + \mathbf{V}\cdot\nabla q = a_q\left(\frac{q_s-q}{\Delta\tau}\right), \tag{18}$$

where the proportionality factors a_θ, a_q are independent of pressure; they may vary in time depending on the particular form of the parameterization scheme. The relationship of these generalized structure functions to the apparent heat source Q_1 and the apparent moisture sink Q_2 are

$$Q_1 = a_\theta\left[c_p\frac{T}{\theta}\frac{(\theta_s-\theta)}{\Delta\tau} + \omega c_p\frac{T}{\theta}\frac{\partial\theta}{\partial p}\right] + c_p\frac{T}{\theta}H_R, \tag{19}$$

$$\frac{Q_2}{L} = -a_q\left(\frac{q_s-q}{\Delta\tau}\right) - \omega\frac{\partial q}{\partial p}. \tag{20}$$

Furthermore, the proportionality factors a_θ, a_q are related to the moisture convergence via the relations

$$a_\theta = \frac{I_\theta}{Q_\theta} = \frac{I(1-b)}{Q_\theta} = I_L(1+\eta)(1-b)/Q_\theta, \tag{21}$$

$$a_q = \frac{I_q}{Q_q} = \frac{Ib}{Q_q} = \frac{I_L(1+\eta)b}{Q_q}. \tag{22}$$

Thus, if b and η are determined, then the functions a_θ and a_q are known and the parameterization is closed.

In this context it is important to recognize a limiting case of Kuo scheme 1, the ultimate Kuo scheme, which is constructed diagnostically from exact estimates of a_θ and a_q. Because of the inherent limitations of the structure functions $q_s - q$ and $\theta_s - \theta$ even this exact knowledge of a_θ and a_q cannot reproduce the correct vertical distributions of the apparent heating and cooling.

a. The ultimate Kuo scheme

Here the starting point of the analysis is the so-called observed estimates of Q_1 and Q_2 from the Ooyama-Esbensen-Chu (1977)[1] data sets described in Section 3. Upon vertical integration of the above equations we obtain

$$a_\theta = \frac{\bar{Q}_1(p_B-p_T)/g}{\frac{1}{g}\int_{p_T}^{p_B} c_p\frac{T}{\theta}\left(\frac{\theta_s-\theta}{\Delta\tau} + \omega\frac{\partial\theta}{\partial p}\right)dp} = \frac{\bar{Q}_1(p_B-p_T)/g}{Q_\theta},$$

$$a_q = -\frac{\frac{\bar{Q}_2}{L}\frac{(p_B-p_T)}{g} + \frac{1}{g}\int_{p_T}^{p_B}\omega\frac{\partial q}{\partial p}dp}{\frac{1}{g}\int_{p_T}^{p_B}\left[\frac{q_s-q}{\Delta\tau}\right]dp}, \tag{23}$$

where

$$Q_q = \frac{1}{g}\int_{p_T}^{p_B}\left[\frac{q_s-q}{\Delta\tau}\right]dp,$$

$$a_q = -\frac{\frac{\bar{Q}_2}{L}\frac{(p_B-p_T)}{g} - I_L}{Q_q}. \tag{24}$$

Here the overbar denotes a vertical average between p_T and p_B. The limits of the integrals are from p_T to p_B.

The above relations are used to obtain the values of a_θ and a_q during the entire third phase of gate. Since Q_1, Q_2, Q_q, Q_θ and I_L vary in time, the proportionality factors a_θ and a_q in this ultimate Kuo formulation also vary with time. The next step in this analysis is a determination of the apparent heating $Q_1(p, t)$ and moistening $Q_2(p, t)$ based on these best

[1] The Ooyama-Esbensen-Chu data sets, referenced in this paper, for phase III of GATE were made available to us by Dr. J. H. Chu of the Space Science and Engineering Center, University of Wisconsin, Madison.

estimates of a_θ, a_q. This is done by simply using the best estimates in (19) and (20). It is obvious that these estimates of Q_1 and Q_2 on the vertical time sections would not necessarily be in agreement with those obtained from the direct use of observations, since the structures of the moistening and heating are not as simple as $q_s - q$ and $\theta_s - \theta$. These structures of $Q_1(p, t)$ and $Q_2(p, t)$ serve as a benchwork for various prognostic formulations of the Kuo schemes, and no improvement beyond these depictions would be possible for this choice of the vertical structure functions. A comparison of the observed and the ultimate Kuo scheme is presented in Section 4.

It should be noted that this scheme is purely diagnostic and cannot be used in forecast models, since it presupposes a knowledge of the exact estimates of a_θ and a_q.

b. A multiple regression approach for finding the parameters a_θ, a_q

This is a prognostic formulation where the mesoscale convergence parameter η and the moistening parameter b are expressed as functions of pairs of known various large-scale variables such as vertical velocity, divergence, vertical shear of the horizontal wind, vorticity, $T_s - T$, $q_s - q$, etc. Among these pairs the vertically averaged large-scale vertical velocity $\bar{\omega}$ and the 700 mb relative vorticity ζ were found to provide the best estimates of heating and moistening with respect to the ultimate Kuo scheme. The design of this regression approach for prognostic models is as follows. We first express the vertically averaged moistening and heating via the linear regression relations

$$\frac{M}{I_L} = a_1\zeta + b_1\bar{\omega} + c_1, \tag{25}$$

$$\frac{R}{I_L} = a_2\zeta + b_2\bar{\omega} + c_2, \tag{26}$$

where the coefficients a, b and c of the planar regression are determined from 72 map times of the GATE observations. Here the time series of

$$\frac{M}{I_L} = -\frac{Q_2 + I_L}{I_L}$$

and R/I_L are known from the observations of Ooyama-Esbensen-Chu and Hudlow and Patterson (1979). A standard procedure for a least-square planar multiple regression is used to determine these coefficients. Here we noted that it is advantageous to work with the departures from the time averages of Q_2/I_L, R/I_L, $\bar{\omega}$ and ζ, and the averages absorbed after the fact with the coefficients c_1 and c_2. The regression based on 72 map times of data gave the relations

$$\frac{-Q_2 + I_L}{I_L} = 0.158 \times 10^5\zeta + 0.304 \times 10^3\bar{\omega} + 0.476, \tag{27}$$

$$\frac{R}{I_L} = 0.107 \times 10^5\zeta + 0.107 \times 10^3\bar{\omega} + 0.870. \tag{28}$$

It may be noted that the left-hand side of the above expressions are dimensionless, while ζ and $\bar{\omega}$ have dimensions of s^{-1} and mb s^{-1}, respectively. The constants have the following dimensions:

$a_1 = 0.158 \times 10^5$ s

$b_1 = 0.304 \times 10^3$ mb^{-1} s

$c_1 = 0.476$ (dimensionless)

$a_2 = 0.107 \times 10^5$ s

$b_2 = 0.107 \times 10^3$ mb^{-1} s

$c_2 = 0.870$ (dimensionless).

The multiple regression does not explicitly state that the rainfall rate is a direct function of upward vertical velocity. It is the ratio R/I_L which is regressed against the relative vorticity and the vertically averaged vertical velocity. The constant term in the regression has a dominant role in this analysis. To a first approximation, the rainfall rate R is equal to the large-scale moisture convergence I_L. This equality would require the constant to be equal to 1 and the coefficient of ζ and $\bar{\omega}$ be equal to 0. That, of course, describes the Kuo (1974) scheme with a setting of $b = 0$. In trying to fit the rainfall data to the parameters I_L, ζ and $\bar{\omega}$, we are working with a relation

$$R = 0.870I_L + 0.107 \times 10^3\omega I_L + 0.107 \times 10^5\zeta I_L. \tag{29}$$

This regression states that for a given large-scale moisture supply I_L, large-scale vertical motions ($\omega < 0$) diminish the rainfall rates while large cyclonic relative vorticity adds to the rainfall rates. The two terms on the right-hand side provide a fine tuning of the rainfall estimates beyond $R = I_L$. It is not the intention of this paper to provide a physical interpretation of the rainfall (or the analogous moistening) regression relations. In practical application of this scheme, the coefficient of ζ should take an opposite sign in the Southern Hemisphere and should be set to zero along the equator. Since ω is usually of the order of 10^{-3} mb s^{-1} and ζ is of the order of 10^{-4} s^{-1}, the moistening or heating do not exhibit any strong bias toward either ζ or ω in the multiple regression. Thus, the need for multiple regression as against linear regression appeared quite worthwhile.

We next determine η and b from solution of the equations

$$(1 + \eta)b = a_1\zeta + b_1\bar{\omega} + c_1, \quad (30)$$

$$(1 + \eta)(1 - b) = a_2\zeta + b_2\bar{\omega} + c_2, \quad (31)$$

i.e.,

$$b = \frac{a_1\zeta + b_1\bar{\omega} + c_1}{(a_1 + a_2)\zeta + (b_1 + b_2)\bar{\omega} + (c_1 + c_2)}, \quad (32)$$

$$\eta = [(a_1 + a_2)\zeta + (b_1 + b_2)\bar{\omega} + (c_1 + c_2)] - 1, \quad (33)$$

where a_θ and a_q are now determined from the relations

$$a_\theta = \frac{I_L(1 - b)(1 + \eta)}{Q_\theta} = \frac{I_L}{Q_\theta}(a_2\zeta + b_2\bar{\omega} + c_2), \quad (34)$$

$$a_q = \frac{I_L b(1 + \eta)}{Q_q} = \frac{I_L}{Q_q}(a_1\zeta + b_1\bar{\omega} + c_1). \quad (35)$$

This is a prognostic scheme, i.e., it provides measures of the moistening, heating and rainfall rates as a function of the evolving fields of $\bar{\omega}$ and ζ. The coefficients a_1, b_1, c_1, a_2, b_2 and c_2 have fixed values for all applications.

We note that a_θ and a_q vary in time, their variations being determined by a function space—the functions being $\bar{\omega}$ and ζ which exhibit considerable variations in time; thus, we expect reasonable application of this scheme beyond the geographical domain of the GATE B-scale array. In Section 4, we shall present a comparison of results of heating, moistening and rainfall rates derived from this scheme with the observed and ultimate Kuo schemes.

c. *The Kuo (1974) scheme*

An investigation of this method was carried in part I of this study. In that study we noted that a vanishingly small value of b ($b \approx 0$) provided the best measures of rainfall rates during the third phase of GATE. This method corresponds to a substitution of $\eta = 0$, $b = 0$ in the aforementioned analysis. This scheme has found wide application in global numerical weather prediction (Krishnamurti *et al.*, 1981; Shaw, 1981). Fig. 1 illustrates the observed and predicted GATE rainfall rates from this method. The predictions here are called the semi-prognostic estimates based on single time prediction from this scheme. The correspondence between the observed and predicted magnitudes is quite reasonable. With the choice of $b = 0$ and $\eta = 0$ the following relations hold:

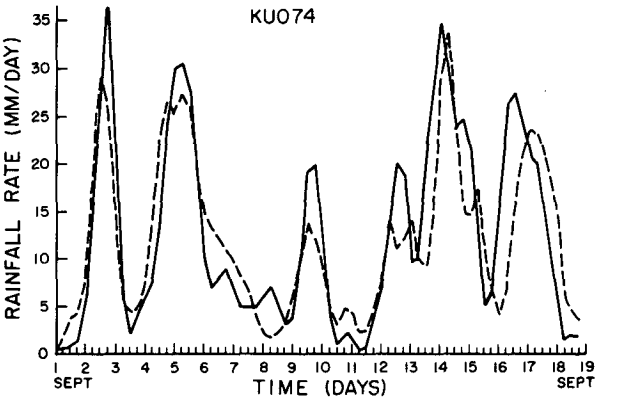

FIG. 1. Comparison of observed (solid line) and predicted (dashed line) rainfall rates (mm day^{-1}) using Kuo's (1974) scheme. Days 1–18 correspond to Phase III of GATE between 1 and 18 September 1974. Data are for 6 h intervals beginning with 0000 GMT 1 September.

$$I_q = 0, \quad (36)$$

$$a_q = 0, \quad (37)$$

$$I_\theta = I_L, \quad (38)$$

$$a_\theta = I_L/Q. \quad (39)$$

Thus a major defect of this scheme is that no moistening is permitted and all of the available large-scale supply of moisture I_L goes into heating. A comparison of the calculated field of the apparent heat source Q_1 for this scheme with those obtained from the observations of Ooyama *et al.* (1977) and from the ultimate Kuo scheme is presented in Section 4. In practical application the lack of moistening would lead to considerable drying of the atmosphere. This has been circumvented by a choice of large vertical diffusion coefficients in the moisture conservation equation. That has the drawback that it allows for strong downgradient fluxes in both moist as well as dry areas and does not have the selective role of pumping of moisture in convective areas alone.

d. *The classical Kuo (1965) scheme*

Here the structure functions for heating and moistening are multiplied by a constant. It can be viewed in the generalized context presented in Section 2b by setting

$$\eta = 0, \quad (40)$$

$$b = Q_q Q^{-1}, \quad (41)$$

$$= \frac{\frac{1}{g}\int_{p_T}^{p_B} \frac{q_s - q}{\Delta\tau}\, dp}{\frac{1}{g}\int_{p_T}^{p_B} \frac{q_s - q}{\Delta\tau}\, dp + \frac{1}{g}\int_{p_T}^{p_B}\left(\frac{c_p T(\theta_s - \theta)}{L\theta\Delta\tau} + \frac{\omega c_p T}{L\theta}\frac{\partial\theta}{\partial p}\right)dp}. \quad (42)$$

TABLE 2. List of symbols.

Symbol	Meaning of the symbol
a_θ	partitioning factor for potential temperature
a_q	partitioning factor for specific humidity
a_1, b_1, c_1	coefficients of the multi-regressed planar surface of the ratio of the rainfall rate to the large-scale supply of moisture
a_2, b_2, c_2	coefficients of the multi-regressed planar surface of the ratio of the moistening rate to the large-scale supply of moisture
b	moistening parameter
C_p	specific heat of air at constant pressure
$\bar{c}$	condensation
$\bar{e}, E$	evaporation
F_q	vertical latent heat flux by the subgrid scale
F_s	vertical sensible heat flux by the subgrid scale
H_c	convective heating rate
H_R	total radiative potential temperature change rate (°C s^{-1})
I, I_G, I_q	total supply of moisture and its partitioning
I_L	large-scale supply of moisture
L	latent heat of condensation
M	moistening rate
P	precipitation
P_T	pressure at cloud top
P_B	pressure at cloud base
p	pressure
q	specific humidity
q_s	saturation specific humidity
Q, Q_θ, Q_q	supply of moisture and the partitioning of Q
Q_1	apparent heating
Q_2	apparent moistening
R	rainfall rate
S	static energy
T	temperature
T_s	temperature of a local moist adiabat
t	time
$\mathbf{V}$	horizontal wind vector
ω	vertical p-velocity
$\bar{\omega}$	mean tropospheric vertical velocity
ζ	lower tropospheric relative vorticity
η	mesoscale convergence parameter
$\Delta\tau$	cloud time scale (20 min)
∇	horizontal vector gradient operator.

This leads to the following relations:

$$I_q = I_L b \tag{43}$$

$$= \frac{I_L Q_q}{Q}, \tag{44}$$

$$I_\theta = (1 - b) I_L \tag{45}$$

$$= \frac{Q - Q_q}{Q} I_L \tag{46}$$

$$= \frac{I_L Q_\theta}{Q}. \tag{47}$$

Thus, we obtain

$$\frac{I_q}{Q_q} = \frac{I_\theta}{Q_\theta} = \frac{I_L}{Q} = \frac{I}{Q}. \tag{48}$$

Furthermore, following Kuo (1965), if we define

$$a = IQ^{-1}, \tag{49}$$

then we note that $a_\theta = a_q = a$. Thus, the prognostic equations for this system become

$$\frac{\partial \theta}{\partial t} = -\mathbf{V} \cdot \nabla\theta - \omega \frac{\partial \theta}{\partial p} + a\left[\omega \frac{\partial \theta}{\partial p} + \left(\frac{p_0}{p}\right)^{R/c_p} \frac{(T_s - T)}{\Delta\tau}\right], \tag{50}$$

$$\frac{\partial q}{\partial t} = -\mathbf{V} \cdot \nabla q + a\left(\frac{q_s - q}{\Delta t}\right). \tag{51}$$

The corresponding rainfall rate is given by

$$R = \frac{c_p}{Lg} \int_{p_T}^{p_B} a\left[\omega\left(\frac{T}{\theta}\right)\frac{\partial \theta}{\partial p} + \frac{(T_s - T)}{\Delta\tau}\right] dp. \tag{52}$$

This classical scheme has been widely used in hurricane models and in large-scale numerical weather prediction. It was shown in part I of this paper that this method underestimates the rainfall rates considerably, although the phase of the maximum rainfall episodes during GATE is reasonably reproduced. The vertical distribution of apparent heat source and apparent moisture sink for this scheme may be expressed by

$$Q_1 = a\left(c_p \frac{T}{\theta}\frac{\theta_s - \theta}{\Delta\tau} + \omega c_p \frac{T}{\theta}\frac{\partial \theta}{\partial p}\right) + c_p \frac{T}{\theta} H_R, \tag{53}$$

$$Q_2 = -L\left(a \frac{q_s - q}{\Delta\tau} + \omega \frac{\partial q}{\partial p}\right). \tag{54}$$

These fields are also compared with the observations and the ultimate Kuo scheme in Section 3.

3. Data sets for the present study

The GATE B-scale data sets are known to be especially high quality for budget studies. Ooyama, Esbensen and Chu have processed this unique data set.

A scale-dependent cubic spline interpolation scheme was used in their analysis to smooth the data in the space-time section of the upper air soundings from various ships. This scheme retains time scales longer than 12 h and vertical wavelengths larger than 100 mb. The analysis scheme is supposed to provide a homogeneity for phenomena in the same region of a wavenumber-frequency domain. Ooyama, Esbensen and Chu used the edited data sets of wind, temperature and humidity to estimate the apparent heat source Q_1 and the moisture sink Q_2.

These are defined by the usual equations:

$$Q_1 = c_p\left(\frac{\partial \bar{T}}{\partial t} + \mathbf{V}\cdot\nabla\bar{T}\right) + \bar{\omega}\frac{\partial \bar{S}}{\partial p} \tag{55}$$

$$= Q_R + L(\bar{c} - \bar{e}) + \frac{\partial}{\partial p} gF_s \tag{56}$$

(a list of symbols is provided in Table 2) and

$$Q_2 = -L\left(\frac{\partial \bar{q}}{\partial t} + \mathbf{V}\cdot\nabla\bar{q} + \bar{\omega}\frac{\partial \bar{q}}{\partial p}\right) \tag{57}$$

$$= L(\bar{c} - \bar{e}) - L\frac{\partial}{\partial p} gF_q. \tag{58}$$

Here the overbar denotes an average over the GATE B-scale, and F_s and LF_q denote vertical fluxes of sensible and latent heat by the subgrid-scale (smaller than B-scale here) motions. These estimates enable us to determine the so-called "observed measures" of Q_1 and Q_2 as a function of pressure and time for the entire third phase of GATE. This covers the first 18 days during September 1974. The vertical resolution of these data is 25 mb and the horizontal resolution 10^5 km^2 which is the approximate area of the GATE B-scale array; the time resolution of this data is 6 h. Q_1 and Q_2 are here calculated from the large-scale observations of $\bar{T}$, $\bar{\mathbf{V}}$, $\bar{S}$ (the dry static energy), $\bar{q}$ and $\bar{\omega}$. These calculations are purely diagnostic in that the time tendency terms are evaluated from observations.

Radiative effects

Cox and Griffith (1979a,b) have made some of the best estimates of the shortwave and longwave radiative divergence fields during the third phase of GATE. Their methodology consists of determining from satellite and radar the cloud structures during the entire period. In addition, the infrared outgoing irradiances and the albedo at the top of the atmosphere are inferred from the satellite observations. These in turn provide the upper boundary condition for calibrating the shortwave and longwave irradiance algorithms. The irradiance calculations utilize the 6 h soundings of temperature and humidity from the GATE ships. The calculations provide a measure of radiative diurnal changes over the GATE array. Table 3 from their study illustrates the 6 h averaged net radiating heating (or cooling) rates averaged over the entire third phase of GATE. It is apparent from this data set that the magnitude of the net radiation changes a lot between night and daytime hours over the entire troposphere. In addition to this, we also had available the daily mean profiles of net radiation for the entire third phase of GATE. The final radiation fields $H_R(p, t)$ used in the present study include a sum of the Phase III mean values and the diurnal variability illustrated in Table 3. Thus, only four vertical profiles of net radiation (6 h apart) are used here; however, we feel that this provides a considerable improvement over the climatological estimates, such as those of Dopplick (1972) which have been used most extensively in a number of budget studies.

4. Computational results

a. Vertical distribution of apparent heating (Q_1)

In Figs. 2a–2e, the following apparent heating fields for the third phase of GATE are shown on vertical time sections: observed field (Fig. 2a); ultimate Kuo scheme (Fig. 2b); multiple regression approach (Fig. 2c); the Kuo (1974) method with b (the moistening parameter) = 0 (Fig. 2d); the classical Kuo (1965) method (Fig. 2e).

All of the above results are here expressed in units of °C day^{-1}. The large observed heating occurred during wave passages during September 1974 on the following dates: 2, 3, 5, 6, 12, 13, 14, 16, 17. The maximum value of heating lies between 10 and 20°C day^{-1}. The level of maximum heating is generally located near the 500 mb level, although on some occasions, e.g., on the 13, 14 and 16 September, the level of maximum heating was close to 750 mb. Except for few occasions this field is generally positive at all levels.

The ultimate Kuo scheme (Fig. 2b) is constructed on the assumption that the exact value of the vertically integrated heating is known and its vertical dis-

TABLE 3. Six-hourly total radiative values (°C day^{-1}) averaged over the entire Phase III period.

Pressure level (mb)	Time (GMT)			
	0000–0600	0600–1200	1200–1800	1800–2400
100	−0.78	−0.09	−0.10	−0.74
175	−0.93	−0.14	−0.15	−0.92
250	−1.52	−0.31	−0.34	−1.55
325	−2.02	−0.29	−0.36	−2.14
400	−2.34	−0.40	−0.47	−2.43
475	−2.55	−0.58	−0.59	−2.52
550	−2.70	−0.76	−0.70	−2.56
625	−2.36	−0.79	−0.72	−2.24
700	−2.08	−0.89	−0.83	−2.01
775	−1.81	−0.93	−0.89	−1.79
850	−1.46	−0.80	−0.79	−1.46
925	−1.04	−0.49	−0.48	−1.03
1000	−0.10	−0.10	−0.12	−0.12

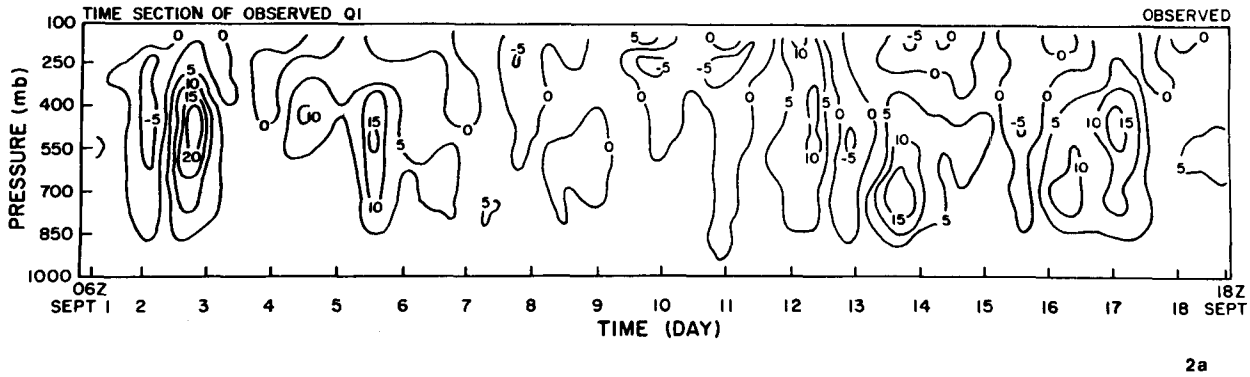

FIG. 2a. Vertical cross section of the apparent heat source Q_1 (°C day^{-1}). Abscissa denotes dates during Phase III of GATE, with data at 6 h intervals. The vertical coordinate is pressure.

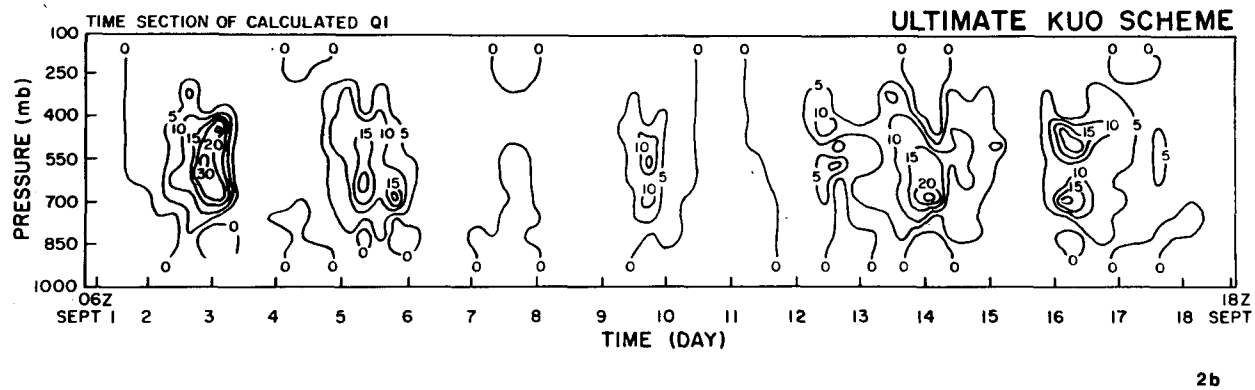

FIG. 2b. As in Fig. 2a except for the apparent heat source Q_1 for the ultimate Kuo scheme.

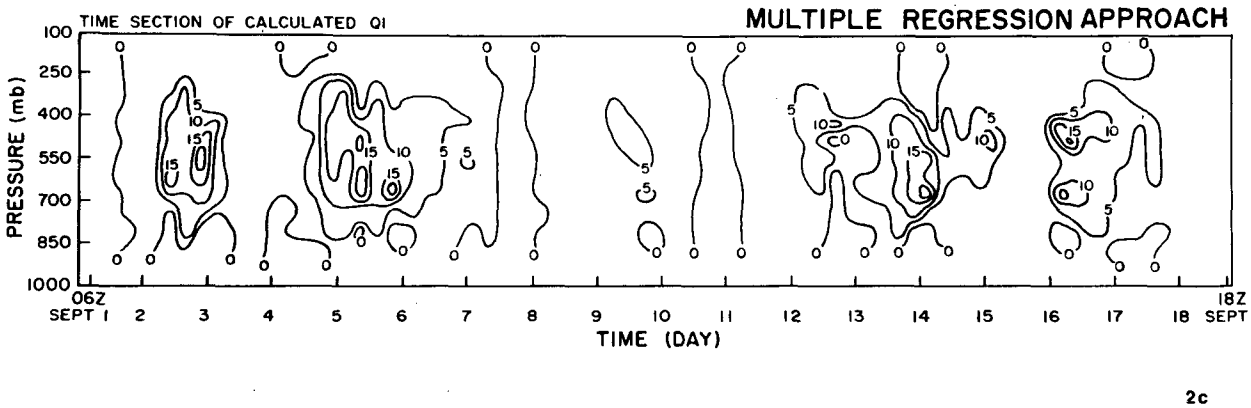

FIG. 2c. As in Fig. 2a except for the apparent heat source Q_1 for the multi-regression approach.

tribution is proportional to $T_s - T$ which makes it difficult from the observed distribution shown in Fig. 2a. This structure function, which is common to all Kuo schemes presented here, has a sharper increase and decrease of the heating along the vertical compared to the observed field. The maximum values of the heating are thus somewhat larger for the ultimate Kuo scheme and they generally occur near the 600 mb level which is somewhat lower than the observed maxima. Because of the sharper vertical gradient the heating for the ultimate Kuo scheme falls off, in general, to values below 5°C day^{-1} above the 350 mb level. Thus, the heating is small between 200 and 300 mb. There are no phase errors in this representation because of the constraint in the vertical integral.

The results of the multiple regression approach,

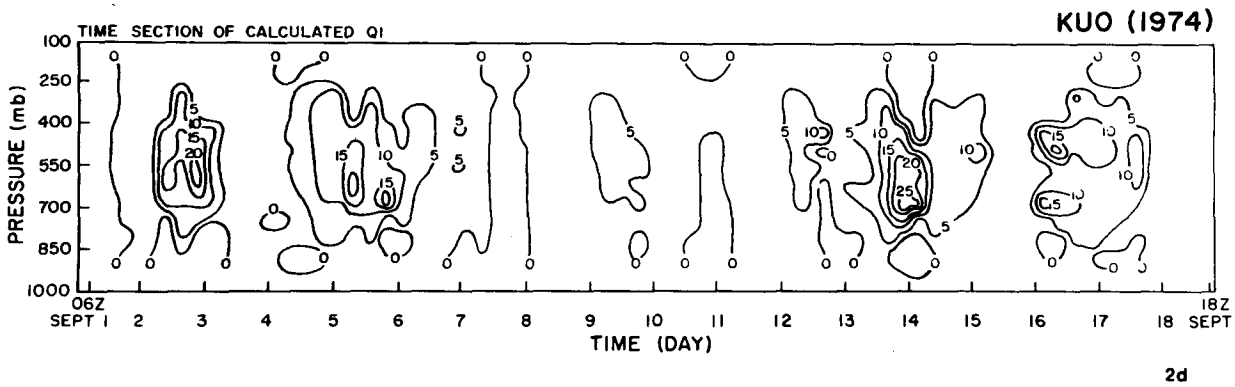

FIG. 2d. As in Fig. 2a except for the apparent heat source Q_1 for the Kuo (1974) scheme for a choice of $\eta = 0$ and $b = 0$.

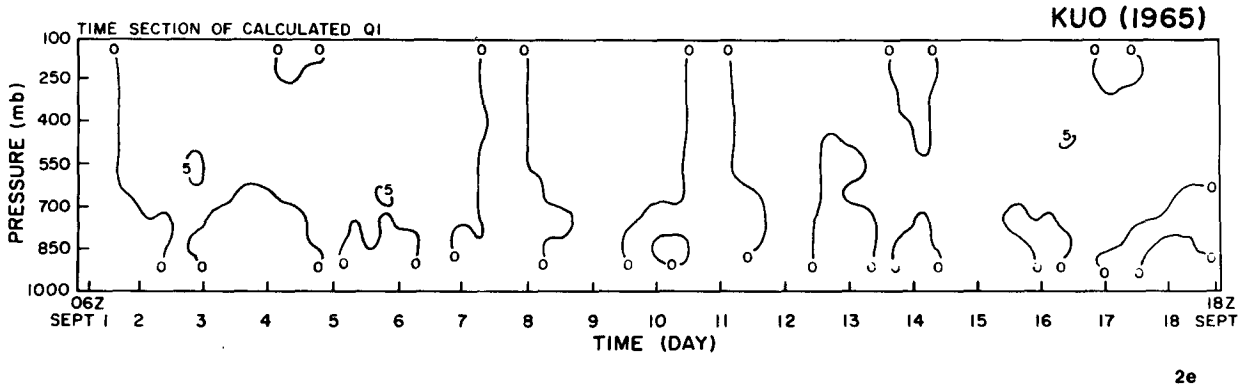

FIG. 2e. As in Fig. 2a, except for the apparent heat source Q_1 for the classical Kuo (1965) scheme.

presented in Fig. 2c, are obtained from a prognostic scheme and are not constrained by the observed vertical integrals of heating. Maximum heating occurs on 2, 3, 5, 6, 12, 13, 14, 16, and 17 September. These are identical to the observed periods of maxima seen in Fig. 2a. The maximum values of heating are $\sim 15°C\ day^{-1}$ and are close to the observed magnitudes shown in Fig. 2a. Figs. 2a, 2b and 2c all show good agreement with respect to each other. This lends credence to the choice of the vertically integrated vertical velocity and the lower tropospheric relative vorticity for defining the heating and moistening via multiple regression. The field shown in Fig. 2c underestimates the heating just below the tropopause level, such a behavior analogous to that for the ultimate Kuo's scheme. We believe that this cannot be improved with the present choice of the structure function $(T_s - T)$. The heating for the Kuo (1974) scheme (Fig. 2d) arrived at by setting $b = 0$ and $\eta = 0$, is also very realistic. This is not surprising since this scheme is known, as indicated in part I, to show good agreement for the vertically integrated heating and the rainfall rates. Some of the maximum values of heating such as those around 3 and 14 September were slightly overestimated by this scheme. The multiple regression approach (Fig. 2c), on the other hand, does not exhibit any such large values. Overall, the heating distribution from Kuo (1974) shown in Fig. 2d is quite impressive. This method, as stated earlier, is not very useful because of its major limitations in its description of moistening. Finally, Fig. 2e shows the distribution of apparent heating for the classical Kuo (1965) scheme. As noted in I, this underestimates the vertical distribution of heating, i.e., most of the heating rates are less than $5°C\ day^{-1}$. The rainfall estimates from this scheme are about 20% of the observed magnitudes, as shown in I.

b. Vertical distribution of the apparent moisture sink (Q_2)

The results of these calculations are shown in Figs. 3a–3d. The four parts present the vertical time sections of the apparent moisture sink from (a) GATE observations, (b) the ultimate Kuo scheme, (c) the present multiple regression approach, and (d) the classical Kuo (1965) scheme. Not shown in this list of panels is the moistening for the Kuo (1974) scheme since its choice of $b = 0$ sets the moistening to zero, as shown in Eq. (37). The observed field of the apparent moisture sink shown in Fig. 3a exhibits large drying ($Q_2 > 0$) during episodes of disturbance pas-

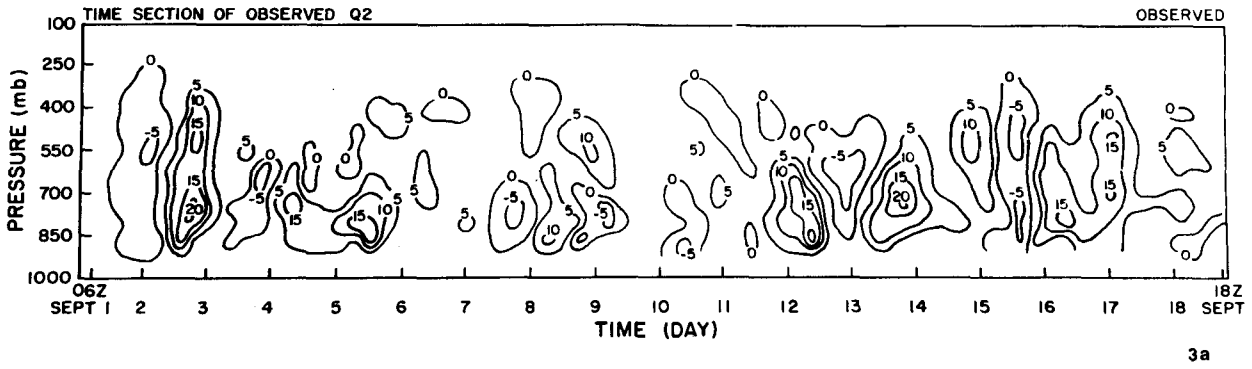

FIG. 3a. Vertical cross section of the apparent moisture sink Q_2 (°C day^{-1}). Abscissa denotes dates during Phase III of GATE, with data at 6 h intervals. The vertical coordinate is pressure.

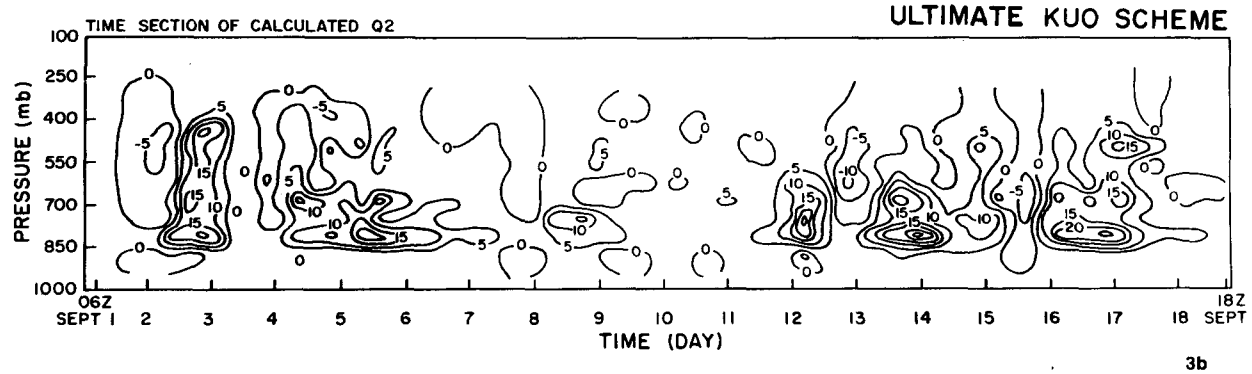

FIG. 3b. As in Fig. 3a except for the apparent moisture sink Q_2 for the ultimate Kuo's scheme.

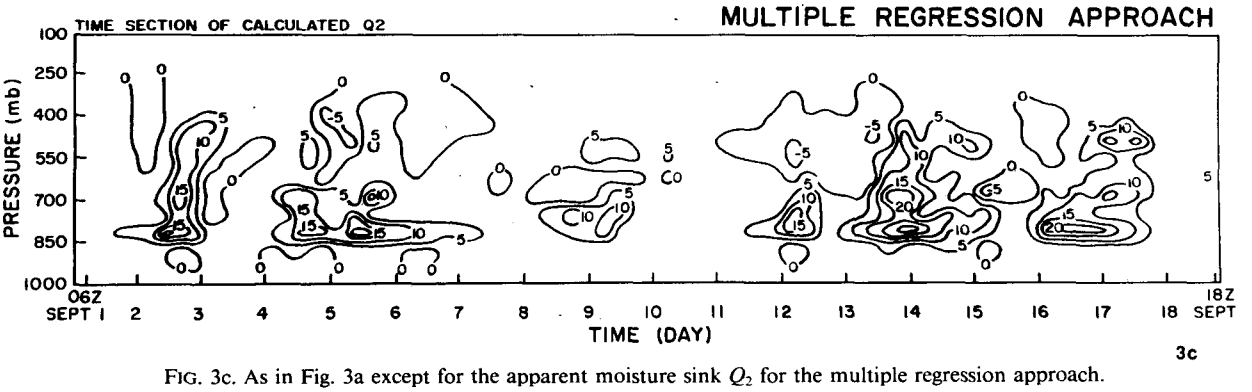

FIG. 3c. As in Fig. 3a except for the apparent moisture sink Q_2 for the multiple regression approach.

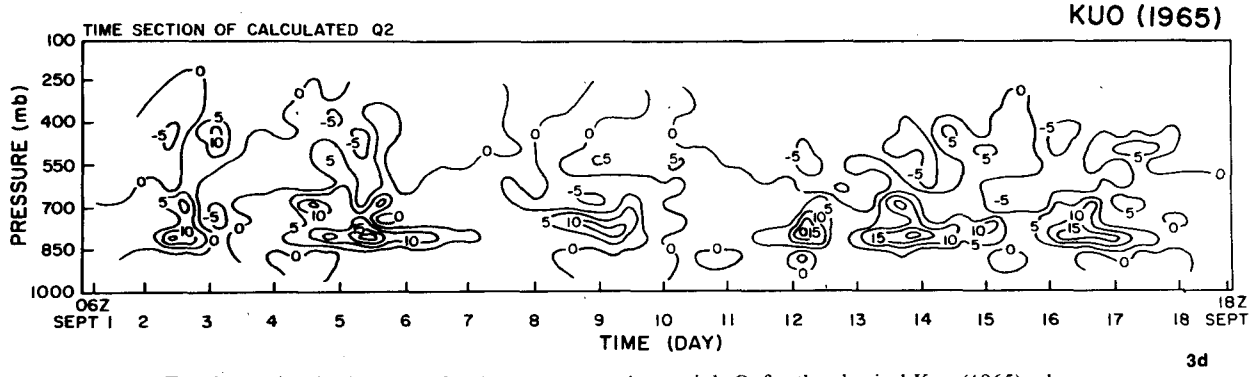

FIG. 3d. As in Fig. 3a except for the apparent moisture sink Q_2 for the classical Kuo (1965) scheme.

sages, i.e., over the periods 2–3, 5–6, 8–9, 12–14 and 16–17 September. The maximum intensity of this drying is of the order of 15°C day^{-1}. In general, the largest amplitude of drying occurs around and below 700 mb. Occasionally, it extends to very high levels in the troposphere, e.g., on 2–3 and 16–17 September. The period of strong drying ($Q_2 > 0$) usually occurs soon after a period of strong moistening ($Q_2 < 0$).

The period of strong drying usually coincides with the periods of strong apparent heating. The period of moistening is interpreted as a cloud build-up stage when a gradual growth of convective cloud occurs, the subgrid-scale (smaller cumulus) contributes to the initial moistening, and the subsequent drying is usually attributed to the strong downdrafts.

The results for the ultimate Kuo scheme (shown in Fig. 3b) essentially capture all of the observed features of an apparent moisture sink. There is, however, a systematic tendency for larger drying to occur near the 800 mb level instead of 700–750 mb as in the observed fields. This discrepancy appears to be a limitation of the Kuo structure function, although the vertical distribution of Q_2, in general, appears quite close to the observed values. Thus, the structure function does seem to be quite realistic.

The multiple regression approach (shown in Fig. 3c), is based on the use of lower tropospheric relative vorticity ζ and the mean tropospheric vertical velocity $\bar{\omega}$ for defining the moistening distribution. This appears to capture most of the details of the observed distributions of Q_2. Strong apparent moisture sinks ($Q_2 > 0$) between 2–3, 4–5, 9–10, 12–13, 14–15 and 16–17 September are in close agreement with observations. The intensity of drying is somewhat stronger near the 800 mb surface, as was also shown for the ultimate Kuo scheme. The vertical extent of Q_2 over the troposphere is also quite realistic. The obvious shortcoming of this calculation is that it underestimates the moistening ($Q_2 < 0$) just prior to these strong episodes of drying. It is not clear at this stage if this can have any detrimental influence on real data NWP experiments. The evolution of the humidity field largely depends on the specification of Q_2 and the rainfall fields; these seem to be handled quite well by this approach.

Fig. 3d illustrates the field of Q_2 from the classical Kuo (1965) scheme. Here a larger proportion of the available large-scale moisture supply is transferred to moistening than in any other schemes. A comparison of the vertical distribution of Q_2 from Kuo (1965) (Fig. 3d), with that obtained from the multiple regression approach (Fig. 3c), shows that these fields are in fact quite comparable in their structure. This implies that the additional moisture supply, i.e., the mesoscale moisture supply ηI_L, invoked in the multiple regression approach, is largely used for heating. This interpretation is consistent with the finding that in the classical Kuo scheme the heating rates are negligibly small (Fig. 2e). It also implies that the magnitude of η cannot be very small, since the Kuo (1974) scheme utilizes all of the available large-scale I_L (and $\eta = 0$) to provide a reasonable heating. A discussion of the magnitude of η and b are provided in Section 4e.

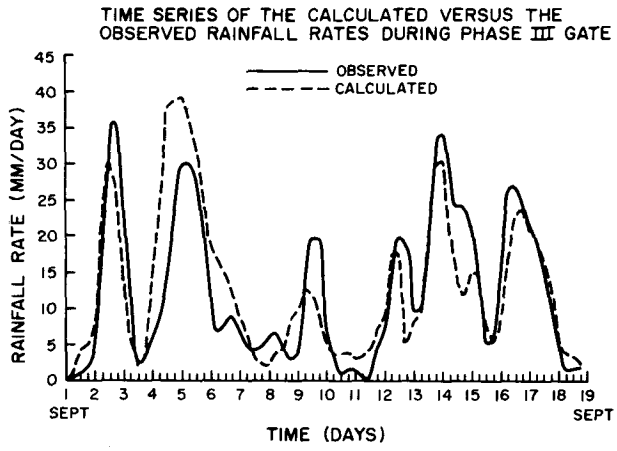

FIG. 4. The observed rainfall rate [from the radar estimates of Hudlow and Patterson (1979)] and those calculated from the multiple regression approach. The ordinate denotes rainfall rate (mm day^{-1}), the abscissa denotes time in 6 h intervals during Phase III of GATE.

c. *Calculated rainfall rates*

Since most of the results of rainfall rates have been presented in I, we shall only show here the newer results for the multiple regression approach (Fig. 4). These are semi-prognostic estimates of the rainfall rates and are obtained from the use of Eqs. (32)–(35) and the prognostic equations. The calculated as well as observed estimates from the Hudlow-Pattersson measurements are shown in this illustration. The one timestep predicted values of rainfall rates are in very close agreement with the observed measures over the GATE B-scale array. As in I we note that the large rainfall episodes (maximum values > 20 mm day^{-1}) during the third phase of GATE around 2–3, 5, 14 and 17 September are related to the passage of squall lines within active African waves. It is interesting to note again, as in I, that the large rainfall amounts from such strong convective systems can be expressed as a function of large-scale variables. This result is implicit in the studies of Thompson *et al.* (1979), Lord (1982), Reeves *et al.* (1979) and many others. The success of this representation (Fig. 4) lies in the unique GATE upper air data sets as well as the unique radar estimates of rainfall rates. We do not believe that such an agreement between observed and calculated estimates would, in general, be possible in the application to most sparse data networks over the tropics.

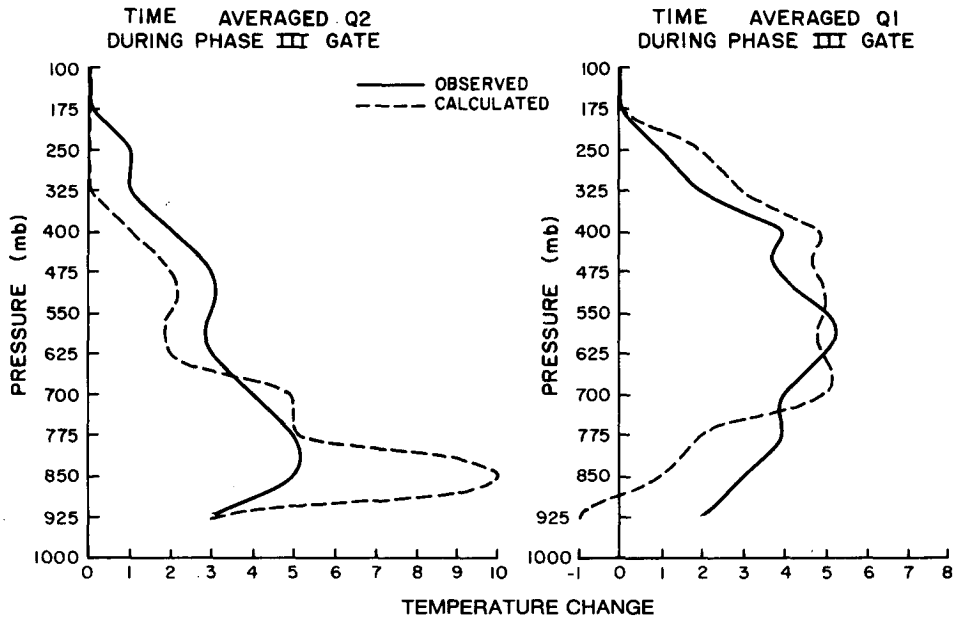

FIG. 5. Time-averaged vertical distributions of the apparent moisture sink Q_2 (left panel) and the apparent heat source Q_1 (right panel). Units are °C day^{-1}. The observed values (solid lines) are compared with those computed from the multiple regression approach (dashed lines).

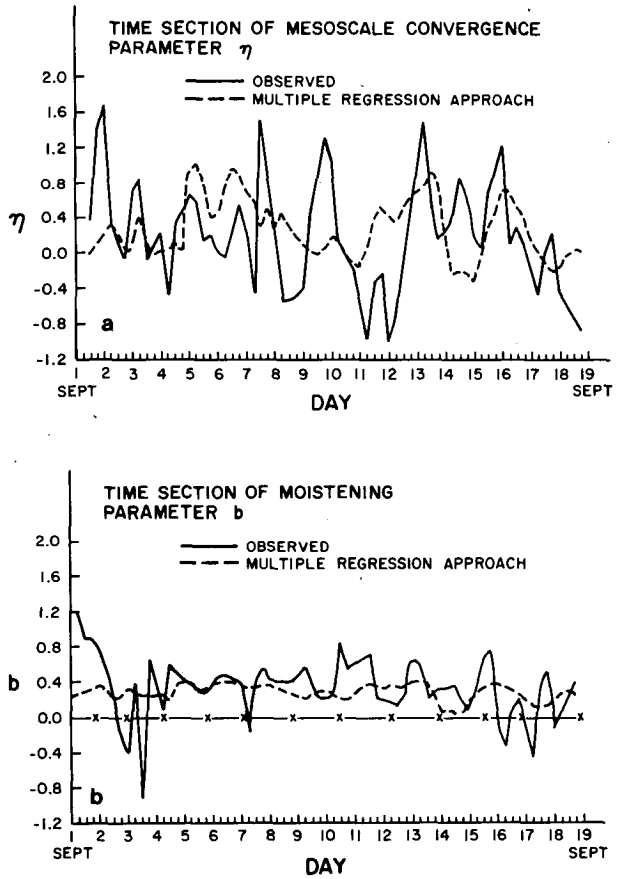

FIG. 6. Time sections of the (a) mesoscale convergence parameter η and the (b) moistening parameter b based on observations (solid lines) and calculated (multiple regression) values (dashed lines).

d. Time-averaged vertical profiles of heating and moistening

Lord (1982) presented time-averaged (for the entire Phase III) vertical profiles of the apparent heat source and moisture sink. A similar representation of the profiles of time-averaged Q_1, Q_2 for the multiple regression approach is presented in Fig. 5. The correspondence between the observed and predicted distributions of the time-averaged apparent heating appears quite reasonable in our study, as well as in Lord's application, which utilizes the Arakawa-Schubert cumulus parameterization scheme. Very close agreement is also noted in the vertical distribution of the apparent moisture sink Q_2 above the 800 mb surface in our study, as well as in Lord's. Both studies, however, show a discrepancy in the predicted values of Q_2 around 850 mb. At this level, both calculations overestimate the drying and slightly underestimate the heating. We believe that the discrepancy could be removed by a planetary boundary layer formulation, one that provides for a large subgrid-scale moistening in disturbed situations.

e. Time evolution of the moistening and mesoscale convergence parameters (b and η)

In Figs. 6a, b we present the time evolution of b and η. The observed time variations of b and η are obtained from the estimates of a_θ and a_q which are given by (23) and (24). A backward substitution of a_θ and a_q into the simultaneous equations (21) and (22) yields solutions for b and η, the two unknowns. The calculated values of b and η are for the multiple

regression approach and are obtained from (32) and (33).

Unlike the earlier schemes where b had been set to a constant and η was set to zero, the time variability, introduced in the new scheme, appears to be a desirable feature. The observed values of b and η do exhibit considerable time variability. The standard deviation of the coefficients by the regression approach were both around 0.6. The mesoscale convergence parameter behaves in an interesting manner during disturbance passage. During periods of heavy rain the magnitude of η is quite large. This implies that mesoscale events are important during disturbed situations and the new cumulus parameterization scheme is able to accommodate this requirement. The calculated amplitude of the mesoscale convergence parameter is not as large as that of the observed magnitude. The curve of the former is somewhat smooth and does not carry as much of the higher frequency details. This is to be expected since η and b are obtained from the regression approach in the function space of $\bar{\omega}$ and ζ which do not carry such high frequencies. In general, the trend of the observed and predicted behavior of η does show a reasonable agreement with a mean value of around 0.4 and a maximum value approaching 1.0.

The moistening parameter b has a mean value of around 0.3. The rainfall rates are about the same for the multiple regression approach and the Kuo (1974) method because $(1 + \eta)(1 - b)$ has nearly the same mean value for the two cases:

Multiple regression: $\eta = 0.4$; $b = 0.3$;
$(1 + \eta)(1 - b) = 0.98$
Kuo (1974): $\eta = 0$; $b = 0$; $(1 + \eta)(1 - b) = 1.0$.

Thus, the rainfall rate R is nearly equal to I_L in both cases. The amplitude of the moistening parameter b is somewhat larger for the observations compared to the predicted estimates. This is again related to the presence of higher frequency information in the observations, while the calculated values are functions of $\bar{\omega}$ and ζ which are more slowly varying in time on the scale of the GATE B-scale array.

5. Concluding remarks

The determination of the vertical distribution of heating and moistening by the cumulus-scale motions and the estimation of reasonable rainfall rates are some of the major problems related to the parameterization of cumulus convection. Reasonable observational estimates of these parameters have been possible from the data sets of Ooyama, Esbensen and Chu for the entire third phase (1–18 September 1974) of the GARP Atlantic Tropical Experiment. These estimates serve as a benchmark for prognostic tests of cumulus parameterization schemes. The recent study of Lord (1982) was a major effort on the application of the Arakawa-Schubert (1974) cumulus parameterization scheme. The present study has explored in detail various aspects of Kuo-type cumulus parameterization schemes. Here, the parameterization is limited by a choice of a structure function for the moistening and heating which are *proportional* to the difference between the cloud and the environmental properties. Within this framework, we have first defined an ultimate Kuo's scheme where the coefficients of *proportionality* are directly obtained from the GATE observations. Although this is not a prognostic scheme, it prescribes an upper limit on the vertical structure of moistening and heating that can be attained by a Kuo-type scheme. The limitations of this ultimate structure are addressed and found to be quite minimal when they are compared with the observational budget estimates.

The main aspect of this paper is a demonstration of the need for mesoscale convergence. This is regarded as a non-measurable subgrid-scale convergence which is quite large during passages of active African waves. The cumulus parameterization is posed as a two-parameter problem: a mesoscale convergence parameter η and a moistening parameter b. The closure of these is attained by a simple planar multi-regression approach. A search of various large-scale parameters shows that the large-scale vertically integrated vertical velocity $\bar{\omega}$ and the lower troposphere relative vorticity ζ can be used as the parameters for regression for the moistening and heating. The regression equations serve as a basis for the development of a cumulus parameterization scheme. The scheme was tested in the semi-prognostic sense to determine the vertical distribution of heating, moistening and rainfall rates for the entire third phase of GATE. The results of these calculations show that the multiple regression approach is capable of predicting these fields with an accuracy quite close to that provided by the ultimate Kuo scheme as well as the observed estimates. Except for a discrepancy at around 800 mb for the drying by the cumulus scale the results show a remarkable degree of success as is evident from Figs. 2c, 3c and 4.

This paper has also addressed a major limitation of the Kuo (1974) scheme for a choice of the moistening parameter $b = 0$. Although this scheme has been used quite extensively in real data numerical weather prediction, it requires the inclusion of a strong vertical diffusion of moisture since the pumping of moisture by the cumulus scale in this case is equal to zero.

Also addressed in this paper are the limitations of the classical Kuo (1965) scheme, for which the obvious underestimates of the heating distribution are mapped.

The prognostic application of these schemes is in preparation, where the results of 96 h real data prediction experiments during GATE are addressed.

Acknowledgments. V. Ooyama, S. Esbensen and J. H. Chu provided the GATE B-scale data sets used in the present study. The research reported here was supported by the Atmospheric Science Section of the National Science Foundation under Grant ATM78-19363. The computations reported here were carried out at the computer facilities at Florida State University and the National Center for Atmospheric Research which is sponsored by the National Science Foundation.

REFERENCES

Arakawa, A., and W. H. Schubert, 1974: Interaction of a cumulus cloud ensemble with the large-scale environment, Part I. *J. Atmos. Sci.*, **31,** 674–701.

Cox, S. K., and K. T. Griffith, 1979a: Estimates of radiative divergence during Phase III of the GARP Atlantic Tropical Experiment. Part I: Methodology. *J. Atmos. Sci.*, **36,** 576–585.

——, and ——, 1979b: Estimates of radiative divergence during Phase III of the GARP Atlantic Tropical Experiment. Part II: Analysis of Phase III results. *J. Atmos. Sci.*, **36,** 586–601.

Dopplick, T. G., 1972: Radiative heating of the global atmosphere. *J. Atmos. Sci.*, **29,** 1278–1294.

Hudlow, M. D., and V. L. Patterson, 1979: *GATE Radar Rainfall Atlas.* Published as a NOAA special report by U.S. Dept. of Commerce. 155 pp.

Kanamitsu, M., 1975: On numerical prediction over a global tropical belt. Rep. No. 75-1, based on Ph.D. dissertation, Dept. of Meteorology, Florida State University, 282 pp.

Krishnamurti, T. N., M. Kanamitsu, R. Godbole, C. B. Chang, F. Carr and J. H. Chow, 1976: Study of monsoon depression II. Dynamical structure. *J. Meteor. Soc. Japan,* **54,** 208–226.

——, H. Pan, C. B. Chang, J. Ploshay and W. Oodally, 1979: Numerical weather prediction for GATE. *Quart. J. Roy. Meteor. Soc.*, **105,** 979–1010.

——, Y. Ramanathan, Hua-Lu Pan, Richard J. Pasch and John Molinari, 1980: Cumulus parameterization and rainfall rates I. *Mon. Wea. Rev.*, **108,** 465–472.

——, Richard Pasch, Hua-Lu Pan, Shao-Hang Chu and Kevin Ingles, 1981: Details of low-latitude medium-range numerical weather prediction using a global spectral model. *Preprints Fifth Conf. Numerical Weather Prediction,* Monterey, Amer. Meteor. Soc., 122–129.

Kuo, H. L., 1965: On formation and intensification of tropical cyclones through latent heat release by cumulus convection. *J. Atmos. Sci.*, **22,** 40–63.

——, 1974: Further studies of the parameterization of the influence of cumulus convection on large-scale flow. *J. Atmos. Sci.*, **31,** 1232–1240.

Lord, S. J., 1980: Verification of cumulus parameterizations using GATE data. *Proc. Seminar on the Impact of GATE on Large-scale Numerical Modeling of the Atmosphere and Ocean.* Nat. Acad. Sci., 276 pp.

——, 1982: Interaction of a cumulus cloud ensemble with the large-scale environment. Part III: Semi-prognostic test of the Arakawa-Schubert cumulus parameterization. *J. Atmos. Sci.*, **39,** 88–103.

Molinari, J., 1982: A method of calculating the effects of deep cumulus convection in numerical models. *Mon. Wea. Rev.*, **110,** 1527–1534.

Reeves, R. W., C. F. Ropelewski and M. D. Hudlow, 1979: Relationships between large-scale motion and convective precipitation during GATE. *Mon. Wea. Rev.*, **107,** 1154–1168.

Shaw, D., 1981: ECMWF operational forecasts in the SW and NE monsoon regions. *Proc. Workshop on Tropical Meteorology and its Effect on Medium Range Weather Prediction at Middle Latitude,* 53–86. [European Centre for Medium Range Weather Forecasts, Shinfield Park, Reading, Berkshire RG2 9AX, Bracknell, England.]

Thompson, R. M., Jr., S. W. Payne, E. E. Recker and R. J. Reed, 1979: Structure and properties of synoptic-scale wave disturbances in the intertropical convergence zone of the eastern Atlantic. *J. Atmos. Sci.*, **36,** 53–72.